

# Randomly accelerated particle in a box: mean absorption time for partially absorbing and inelastic boundaries

Stanislav N. Kotsev and Theodore W. Burkhardt

Department of Physics, Temple University, Philadelphia, PA 19122

(Dated: November 15, 2018)

Consider a particle which is randomly accelerated by Gaussian white noise on the line segment  $0 < x < 1$  and is absorbed as soon as it reaches  $x = 0$  or  $x = 1$ . The mean absorption time  $T(x, v)$ , where  $x$  and  $v$  denote the initial position and velocity, was calculated exactly by Masoliver and Porrà in 1995. We consider a more general boundary condition. On arriving at either boundary, the particle is absorbed with probability  $1 - p$  and reflected with probability  $p$ . The reflections are inelastic, with coefficient of restitution  $r$ . With exact analytical and numerical methods and simulations, we study the mean absorption time as a function of  $p$  and  $r$ .

PACS 02.50.Ey, 05.40.-a, 45.70.-n

## I. INTRODUCTION

Consider a randomly accelerated particle which moves on the half line  $x > 0$  with an absorbing boundary at  $x = 0$ . The motion is governed by

$$\frac{d^2x}{dt^2} = \eta(t) , \quad \langle \eta(t)\eta(t') \rangle = 2\delta(t - t') , \quad (1)$$

where  $\eta(t)$  is uncorrelated white noise with zero mean. The probability  $Q(x, v; t)$  that a particle with initial position  $x$  and initial velocity  $v$  has not yet been absorbed after a time  $t$  has been studied by McKean [1] and others [2, 3, 4]. For a particle initially at  $x = 0$  with velocity  $v > 0$ , the probability decays as

$$Q(0, v; t) \sim \left( \frac{v^2}{t} \right)^{1/4} , \quad t \rightarrow \infty . \quad (2)$$

Following Cornell, Swift, and Bray [5], we consider a more general boundary condition. On arriving at the boundary the particle is absorbed with probability  $1 - p$  and reflected with probability  $p$ . The velocities of the particle just after and before reflection are related by  $v_f = -rv_i$ . Here  $r$  is the coefficient of restitution, and  $r = 1$  and  $r < 1$  correspond to elastic and inelastic collisions, respectively.

As physical motivation, we note that temporal or spatial irregularities at the boundaries of a system or a statistical capture process may give rise to partial absorption. The properties of a particle which is subject to a random force and collides inelastically are of interest in connection with driven granular media.

For the partially absorbing, inelastic boundary condition the probability that the particle has not yet been absorbed decays as

$$Q(0, v; t) \sim \left( \frac{v^2}{t} \right)^{\phi(p, r)} , \quad t \rightarrow \infty . \quad (3)$$

Burkhardt [7] and De Smedt *et al.* [8] showed that the persistence exponent  $\phi(p, r)$  is non-universal, depending on  $p$  and  $r$  according to the relation

$$pr^{2\phi} = 2 \sin \left( \frac{1 - 4\phi}{6} \pi \right) . \quad (4)$$

For  $p = 0$ ,  $\phi(0, r) = \frac{1}{4}$ , so Eqs. (2) and (3) are consistent. Solving Eq. (4) for  $\phi$  graphically, one finds a unique solution  $0 < \phi(p, r) < \frac{1}{4}$  in the physical region  $0 < r < 1$ ,  $0 < p < 1$ , representing a decay slower than in Eq. (2).

The decay in Eq. (3) is so slow that the mean absorption time

$$T(0, v) = \int_0^\infty dt t \left[ -\frac{\partial Q(0, v; t)}{\partial t} \right] = \int_0^\infty dt Q(0, v; t) \quad (5)$$

is infinite, even for  $p = 0$ . On the other hand, the mean absorption time  $T^*(0, v)$ , averaged over a long but finite time  $t^*$  instead of an infinite time, is a well-defined quantity, which varies as

$$T^*(0, v) \sim t^* \left( \frac{v^2}{t^*} \right)^{\phi(p, r)}, \quad t^* \gg v^2 \quad (6)$$

and diverges in the limit  $t^* \rightarrow \infty$ .

If the particle moves on the finite line  $0 < x < 1$  and is absorbed the first time it reaches either  $x = 0$  or  $x = 1$ , the probability that it has not yet been absorbed after a time  $t$  decays as  $e^{-\lambda t}$  for long times [9], much more rapidly than the power law (2) for a single absorbing boundary. The mean absorption time  $T(x, v)$  for a particle with initial position  $x$  and initial velocity  $v$  is well defined. Masoliver and Porrà [10] calculated this quantity exactly, by solving the inhomogeneous Fokker-Planck equation

$$\left( v \frac{\partial}{\partial x} + \frac{\partial^2}{\partial v^2} \right) T(x, v) = -1, \quad (7)$$

with the boundary conditions

$$T(x, v) = T(1 - x, -v), \quad (8)$$

$$T(0, v) = 0, \quad v < 0, \quad (9)$$

corresponding to reflection symmetry and the immediate absorption of a particle with initial conditions  $x = 0, v < 0$ . Their result, which is rederived in the Appendix, is given by

$$\begin{aligned} T_1(x, v) = T_1(1 - x, -v) = & \frac{1}{3}(\pi v)^{1/2} \int_0^{1-x} dy \frac{e^{-v^3/18y}}{y^{1/2}} I_{-1/6} \left( \frac{v^3}{18y} \right) + \frac{2^{-7/3} 3^{5/6}}{\Gamma(2/3)^2} \\ & \times \int_x^1 dy \frac{e^{-v^3/9(y-x)}}{(y-x)^{2/3}} [y(1-y)]^{-1/6} \left[ {}_2F_1\left(1, -\frac{2}{3}; \frac{5}{6}; 1-y\right) - {}_2F_1\left(1, -\frac{2}{3}; \frac{5}{6}; y\right) \right] \end{aligned} \quad (10)$$

for  $v > 0$ , where  ${}_2F_1(a, b; c; z)$  is a standard hypergeometric function [12]. The subscript 1 of  $T_1(x, v)$  is a reminder that the particle is absorbed the first time it reaches either boundary. For use below we note the asymptotic forms

$$T_1(0, v) \sim \begin{cases} \frac{3}{\pi^{1/2}} v^{1/2}, & v \searrow 0 \\ \frac{1}{v}, & v \rightarrow \infty \end{cases} \quad (11)$$

The second of these forms is intuitively obvious, corresponding to ballistic propagation from  $x = 0$  to  $x = 1$  in the time  $v^{-1}$ .

In this paper we study the mean absorption time of a randomly-accelerated particle moving on the finite line  $0 < x < 1$  for the more general boundary condition described above: absorption at the boundary with probability  $1 - p$ , reflection with probability  $p$  and coefficient of restitution  $r$ . For this boundary the mean absorption time also satisfies the Fokker-Planck equation (7) with reflection symmetry (8), but the absorbing boundary condition (9) is replaced by

$$T(0, -v) = pT(0, rv) , \quad v > 0 . \quad (12)$$

The absorbing boundary condition (9) considered by Masoliver and Porrà is unusual in that  $T(0, v)$  is specified for  $v < 0$  but not  $v > 0$ . That the Fokker-Planck equation with this boundary condition and with reflection symmetry (8) is a well-posed boundary value problem was known [11] long before the exact solution of Masoliver and Porrà. We are unaware of a similar proof for the more general boundary condition (12). In this paper we show how to solve the more general case with an extension of the approach of Masoliver and Porrà.

## II. INTEGRAL EQUATION FOR $T(x, v)$

In the Appendix we show that the Fokker-Planck equation (7) with reflection symmetry (8) has the exact Green's function solution

$$T(x, -v) = T_1(x, -v) + \int_0^\infty du u G(x, v, u) T(0, -u) , \quad (13)$$

for  $v > 0$ , where  $T_1$  is the same function as in Eq. (10),

$$G(x, v, u) = \frac{v^{1/2} u^{1/2}}{3x} e^{-(v^3+u^3)/9x} I_{-1/3} \left( \frac{2v^{3/2} u^{3/2}}{9x} \right) - \frac{1}{3^{1/3} \Gamma(\frac{2}{3})} \int_0^x dy \frac{e^{-v^3/9(x-y)}}{(x-y)^{2/3}} [R(y, u) - R(1-y, u)] , \quad (14)$$

$$R(y, u) = \frac{1}{3^{5/6} \Gamma(\frac{1}{3}) \Gamma(\frac{5}{6})} \frac{u^{1/2} e^{-u^3/9y}}{y^{7/6} (1-y)^{1/6}} {}_1F_1 \left( -\frac{1}{6}, \frac{5}{6}, \frac{u^3(1-y)}{9y} \right) , \quad (15)$$

and  ${}_1F_1(a, b, z)$  is a standard confluent hypergeometric function [12].

To calculate  $T(x, -v)$  from Eq. (13), one must first determine the unknown function  $T(0, -u)$  on the right-hand side. Setting  $x = 1$  in Eqs. (13)-(15) and substituting  $T(1, -v) = T(0, v)$  and  $T(0, -u) = pT(0, ru)$ , which follow from Eqs. (8) and (12), leads to the integral equation

$$T(0, v) = T_1(0, v) + p \int_0^\infty du u G(1, v, u) T(0, ru), \quad v > 0, \quad (16)$$

where

$$G(1, v, u) = \frac{1}{6\pi} v^{1/2} u^{1/2} e^{-(v^3+u^3)/9} \left[ \frac{9}{v^3+u^3} + 6 {}_1F_2 \left( 1; \frac{5}{6}, \frac{7}{6}; \frac{v^3 u^3}{81} \right) \right], \quad (17)$$

and  ${}_1F_2(a; b, c; z)$  is a generalized hypergeometric function [12]. Our analytical and numerical predictions for the mean absorption time are derived directly from Eqs. (16) and (17). The same symmetric kernel  $G(1, v, u) = G(1, u, v)$  plays a central role in Refs. [13, 14], in determining the equilibrium distribution function  $P(x, v)$  of a randomly accelerated particle moving between inelastic walls at  $x = 0$  and  $x = 1$  with which it collides inelastically.

As discussed in [14], the quantity  $G(1, v, u)$  generalizes McKean's result for the velocity distribution at first return [15] from the half-line to the finite line. The probability that a randomly accelerated particle, which leaves  $x = 0$  with velocity  $v > 0$ , arrives with speed between  $u$  and  $u + du$  the next time it reaches either  $x = 0$  or  $x = 1$  is given by  $uG(1, v, u)du$ , where the first and second terms of Eq. (17) correspond to arrival at  $x = 0$  and  $x = 1$ , and where

$$\int_0^\infty du u G(1, v, u) = 1. \quad (18)$$

Integral equation (16) follows immediately from this interpretation. The first, second, ... terms in the iterative solution of the integral equation represent the mean time to reach the boundary for the first time, the mean time between the first and second boundary collisions, ..., weighted with a factor  $p$  for each reflection.

In Eq. (16) the asymptotic form of  $T(0, v)$  for small and large  $v$  is determined by the first and second terms, respectively, of the kernel (17). For  $p > 0$  the particle is not always absorbed the first time it reaches the boundary, which implies  $T(0, v) > T_1(0, v)$ . For small  $v$  we look for a solution with the asymptotic form

$$T(0, v) \sim v^\gamma, \quad v \searrow 0, \quad (19)$$

with exponent  $\gamma(p, r)$  smaller than the value  $\gamma = \frac{1}{2}$  for  $p = 0$  in Eq. (11). Substituting Eq.

(19) in Eq. (16), we find that the asymptotic form is consistent with the integral equation if

$$pr^\gamma = 2 \sin \left( \frac{1-2\gamma}{6} \pi \right) . \quad (20)$$

Solving Eq. (20) for  $\gamma$  graphically, one finds a unique solution satisfying  $0 < \gamma(p, r) < \frac{1}{2}$  in the physical region  $0 < r < 1$ ,  $0 < p < 1$ . Comparing Eqs. (4) and (20), one sees that  $\gamma(p, r) = 2\phi(p, r)$ . Thus, the exponents of  $v$  in the results (4), (6) for the half line and (19), (20) for the finite line are the same. This suggests that the small  $v$  behavior (19), (20) is due to repeated collisions with the same boundary.

For large  $v$ ,  $T(0, v) \approx v^{-1} + T(1, v)$ , corresponding to ballistic propagation from  $x = 0$  to  $x = 1$  in the time  $v^{-1}$ . Combining this relation with Eqs. (8) and (12) yields

$$T(0, v) \approx v^{-1} + pT(0, rv) , \quad v \rightarrow \infty . \quad (21)$$

Equation (21) also follows from integral equation (16) on using the asymptotic forms (11) for large  $v$  and  ${}_1F_2\left(1; \frac{5}{6}, \frac{7}{6}; z\right) \approx \frac{1}{6}\pi^{1/2}z^{-1/4}\exp(2z^{1/2})$  for large  $z$ . For  $p < 1$ , the mean absorption time is expected to decrease to zero in the large  $v$  limit. Iteration of Eq. (21) and/or substitution of the ansatz  $T(0, v) \approx Bv^{-\nu}$  in Eq. (21) leads to the asymptotic forms

$$T(0, v) \approx \begin{cases} \frac{r}{r-p} v^{-1} , & p < r \leq 1 , \\ Bv^{-\ln p / \ln r} , & r < p < 1 , \end{cases} \quad (22)$$

for  $v \rightarrow \infty$ , with  $p < 1$ .

The large  $v$  behavior for  $p = 1$ ,  $r < 1$ , corresponding to inelastic reflection with zero absorption probability, requires special attention and is considered in Section V-C.

### III. NUMERICAL SOLUTION OF THE INTEGRAL EQUATION

To interpolate between the asymptotic forms of  $T(0, v)$  for small and large  $v$ , given in the preceding Section, we solved integral equation (16) numerically. Changing the integration variable from  $u$  to  $ru$ , we solved the resulting equation,

$$T(0, v) = T_1(0, v) + \frac{p}{r^2} \int_0^\infty du u G(1, v, r^{-1}u) T(0, u) , \quad v > 0 , \quad (23)$$

by iteration.

To evaluate the integral in Eq. (23) numerically, we changed the integration variable from  $u$  to

$$\begin{aligned} z &= \frac{u^3}{9r^3} , & 0 < u < B , \\ w &= \left( \frac{u^3}{9r^3} \right)^{-\alpha} , & B < u < \infty , \end{aligned} \quad (24)$$

where  $\alpha$  is a positive constant, and then used Simpson's rule, exact for polynomials of degree 3, with equally spaced mesh points in  $z$  and  $w$ . To ensure good accuracy for small  $z$  (small  $u$ ), we subtracted off the leading asymptotic form of the integrand, fit to a power law, and then integrated it analytically. In the region where both  $v$  and  $u$  are small, where the first term in the kernel (17) diverges, the integrand was fit to  $(v^3 + u^3)^{-1}$  times a power law in  $z$  and then integrated analytically. The parameters  $B$  and  $\alpha$  and the mesh size were chosen to give good convergence with about 100 mesh points in each of the intervals  $0 < B < u$  and  $B < u < \infty$ . Starting with  $T_1(0, v)$  as the first approximation to  $T(0, v)$ , one typically needs about 10 iterations for convergence.

#### IV. SIMULATIONS

In our simulations the motion of the particle is governed by the difference equations

$$x_{n+1} = x_n + v_n \Delta_{n+1} + \left( \frac{\Delta_{n+1}^3}{6} \right)^{1/2} (s_{n+1} + \sqrt{3} r_{n+1}) , \quad (25)$$

$$v_{n+1} = v_n + (2\Delta_{n+1})^{1/2} r_{n+1} . \quad (26)$$

Here  $x_n$  and  $v_n$  are the position and velocity at time  $t_n$ , and  $\Delta_{n+1} = t_{n+1} - t_n$ . The quantities  $r_n$  and  $s_n$  are independent Gaussian random numbers such that

$$\langle r_n \rangle = \langle s_n \rangle = 0 , \quad \langle r_n^2 \rangle = \langle s_n^2 \rangle = 1 . \quad (27)$$

As discussed in [16], this algorithm generates trajectories which are consistent with the exact probability distribution  $P(x, v, t)$  of a randomly accelerated particle in free space, i.e. in the absence of boundaries. In free space there is no time step error in the algorithm. The time step  $\Delta_{n+1}$  is arbitrary. However, close to the boundaries trajectories are not generated with the correct probability, because the free space distribution  $P(x, v, t)$  includes trajectories which wander outside the interval  $0 < x < 1$  and return during the time  $t$ . As in [16], we make the time step smaller near the boundaries to exclude these spurious trajectories.

Using the algorithm (25)-(27) with large time steps away from the boundaries, instead of a conventional algorithm with a constant time step, enables us to simulate the particle for much longer times.

For a particle in free space with position and velocity  $x_n, v_n$  at time  $t_n$ , the coordinate  $x_{n+1}$  at a time  $\Delta_{n+1}$  is distributed according to a Gaussian function [16], with a maximum at  $x_n + v_n \Delta_{n+1}$  and root-mean square width  $(\frac{2}{3} \Delta_{n+1}^3)^{1/2}$ . Choosing  $\Delta_{n+1}$  so that

$$x_n + v_n \Delta_{n+1} - c \Delta_{n+1}^{3/2} > 0, \quad (28)$$

$$x_n + v_n \Delta_{n+1} + c \Delta_{n+1}^{3/2} < 1, \quad (29)$$

where the constant  $c$  is about 5 or larger, ensures that the Gaussian distribution lies well within the interval  $0 < x < 1$ .

The largest  $\Delta_{n+1}$  consistent with inequality (28) is given by  $D(x_n, v_n)$ , where

$$x + vD(x, v) - cD(x, v)^{3/2} = 0. \quad (30)$$

To avoid solving Eq. (30), cubic in  $D^{1/2}$ , at each step of the algorithm, one may use the approximation

$$D(x, v) \approx \begin{cases} \left(\frac{x}{c}\right)^{2/3} + \left(\frac{v}{c}\right)^2, & v > 0, \\ \left[\left(\frac{c}{x}\right)^2 - \frac{v}{x}\right]^{-1}, & v < 0, \end{cases} \quad (31)$$

which is asymptotically exact for  $v \rightarrow 0$  and  $v \rightarrow \pm\infty$  and accurate to better than 13% for  $-\infty < v < \infty$ .

The most efficient time step to use in the algorithm is the largest  $\Delta_{n+1}$  consistent with *both* inequalities (28) and (29). Using a smaller  $\Delta_{n+1}$  slows the simulation without improving the accuracy. Since the inequality (29) follows from (28) on making the reflection symmetric substitution  $v_n \rightarrow -v_n, x_n \rightarrow 1 - x_n$ , the optimal time step is

$$\Delta_{n+1} = \text{Min}[D(x_n, v_n), D(1 - x_n, -v_n)] + \delta, \quad (32)$$

where Min denotes the smaller of the two quantities inside the square brackets. As in [16] a small minimum time step  $\delta$  has been included in Eq. (32). Without it, the step size decreases to zero as the particle approaches the boundary, and, as in Zeno's paradox, the particle never gets there. After inclusion of  $\delta$ , the particle not only reaches the boundary but jumps slightly past it. We kept the overshoot small by choosing a sufficiently large value for the parameter  $c$  in Eqs. (28)-(31).



In the case  $p = 1$ ,  $r < r_c$  of highly inelastic collisions with absorption probability zero, the speed of the particle becomes extremely small after many boundary collisions, and great care is required to simulate the behavior reliably. According to Eqs. (26) and (32), the root-mean-square velocity change at each time step has the minimum average value

$$\Delta v = (2\delta)^{1/2}. \quad (33)$$

After each boundary collision we set  $\Delta v$  equal to  $1/500$  of the velocity just after the collision. This  $\Delta v$  is the smallest velocity the algorithm can reliably handle. The corresponding value of  $\delta$ , given by Eq. (33), is then used until the next boundary collision.

The results for the mean time  $T(0, v)$  reported in Section V are based on  $10^4$  independent particle trajectories for each value of the initial velocity  $v$ .

## V. RESULTS

### A. Partially absorbing, elastic boundaries

In this subsection we present our various results for  $p < 1$ ,  $r = 1$ . In this regime the particle is absorbed at the boundary with probability  $1 - p$  and reflected *elastically* with probability  $p$ . This is the “partial survival” model, studied on the half line in Refs. [5, 6, 7, 8].

For  $p < 1$ ,  $r = 1$  the mean absorption time has the asymptotic forms (19), (20), and (22) for small and large  $v$ , respectively. As the reflection probability  $p$  increases from 0 to 1,  $\gamma(p)$  decreases from the Masoliver-Porra result  $\gamma(0) = \frac{1}{2}$  in Eq. (11) for absorption on first arrival at the boundary, to the value  $\gamma(1) = 0$ , corresponding to no absorption at all, or  $T(0, v) = \infty$ .

In Fig. 1 our results for the mean absorption time  $T(0, v)$  for partially absorbing, elastic boundary conditions as a function of the initial velocity  $v$  are compared for  $r = 1$  and  $p = 0.75, 0.5, 0.25, 0$ . The exact asymptotic forms (19) and (20) for small  $v$  and (22) for large  $v$ , the numerical solution of Eq. (16), and the simulation results are clearly in excellent agreement.

For fixed  $v$  the mean absorption time in Fig. 1 increases with increasing reflection probability  $p$ , as expected. For fixed  $p$  the mean absorption time does not vary monotonically with  $v$  but has an absolute maximum at an intermediate velocity. For much larger initial velocities the particle is absorbed more rapidly since it bounces back and forth between

the boundaries, colliding at a rapid rate. For much smaller initial velocities the particle is absorbed more rapidly because it collides repeatedly with the boundary where it starts.

### B. Partially absorbing, inelastic boundaries

Here we present our results for  $p < 1$ ,  $r < 1$ . In this regime the particle is absorbed at the boundary with probability  $1 - p$  and reflected *inelastically* with probability  $p$  and coefficient of restitution  $r$ . Results for the half-line geometry with this boundary condition are given in Ref. [7].

In Fig. 2 our results for the mean absorption time  $T(0, v)$  as a function of the initial velocity  $v$  are compared for  $(p, r) = (0.75, 0.25)$ ,  $(0.501, 0.5)$ , and  $(0.25, 0.75)$ . Again the exact asymptotic forms (19) and (20) for small  $v$  and (22) for large  $v$ , the numerical solution of Eq. (16), and the simulation results are in excellent agreement. Note that the large  $v$  asymptotic forms (22) for  $p < r < 1$  and  $r < p < 1$  are different and that the data test both. Corrections to the large  $v$  asymptotic form in the crossover regime  $p \approx r$  lead to conspicuously slower convergence for  $(p, r) = (0.501, 0.5)$ .

### C. Non-absorbing, inelastic boundaries

In this subsection we consider boundaries with  $p = 1$ ,  $r < 1$ . At the boundary the particle is reflected inelastically with probability 1 and absorbed with probability zero. This is the case of interest in connection with driven granular matter. Cornell *et al.* [5] predicted that for  $r < r_c$ , where

$$r_c = e^{-\pi/\sqrt{3}} = 0.163 \dots, \quad (34)$$

the particle undergoes “inelastic collapse,” making an infinite number of boundary collisions in a finite time, coming to rest, and remaining there.

The prediction that the inelastic collisions localize the particle at the boundary for  $r < r_c$  was questioned by Florencio *et al.* [17] and Anton [18] on the basis of simulations.

The equilibrium distribution function  $P(x, v)$  of a particle moving on the finite line between two inelastic boundaries was studied by Burkhardt, Franklin, and Gawronski [13] for  $r > r_c$  and Burkhardt and Kotsev [14] for  $r < r_c$  with exact analytical and numerical calculations and simulations, similar to this paper. According to [14],  $P(x, v)$  varies smoothly

and analytically with  $r$  throughout the interval  $0 < r < 1$  and does not collapse onto the boundaries. For  $r < r_c$  the equilibrium boundary collision rate is infinite, but the collisions do not localize the particle at the boundary (see footnote [19]).

In the case  $p = 1$ ,  $r < 1$  iterating integral equation (16) adds the mean time to reach the boundary for the first time, the mean time between the first and second boundary collisions, etc., taking the change in speed in each collision into account. Thus the solution  $T(0, v)$  represents the mean time  $T(0, v)$  for an infinite number of boundary collisions.

For  $p = 1$ ,  $r < r_c$ ,  $T(0, v)$  has the asymptotic forms (19), (20) for small  $v$ . As the coefficient of restitution  $r$  increases from 0 to 1,  $\gamma(r)$  decreases from the Masoliver-Porra result  $\gamma(0) = \frac{1}{2}$  in Eq. (11) to the value  $\gamma(r_c) = 0$ , confirming the result of Cornell *et al.* for  $r_c$  in Eq. (34). The negative, unphysical value of  $\gamma$  for  $r > r_c$  signals the breakdown of the solution with finite  $T(0, v)$ . For  $r > r_c$  the mean time for an infinite number of collisions is infinite.

In contrast with the results for  $p < 1$  given in Eq. (22), in the case  $p = 1$ ,  $r < 1$ , the mean time  $T(0, v)$  does not vanish in the limit  $v \rightarrow \infty$ . This may be understood by reverse iteration of the large  $v$  recurrence relation (21), which yields

$$T(0, r^{-n}v) \approx (r + r^2 + \dots + r^n) v^{-1} + T(0, v). \quad (35)$$

This result holds for any finite velocity  $v$  large enough so that the time to travel between the two boundaries is accurately given by the ballistic time  $v^{-1}$ . The first  $n$  terms on the right-hand side give the time a particle with initial velocity  $r^{-n}v$  takes to reach velocity  $v$  and sum to  $r(1 - r)^{-1}v^{-1}$  in the limit  $n \rightarrow \infty$ .

According to Eq. (35),  $\lim_{n \rightarrow \infty} T(0, r^{-n}v) = T(0, \infty)$  is finite and non-vanishing for  $r < r_c$ . The most general asymptotic form for large  $v$  consistent with these two properties and with the recurrence relation (21) is

$$T(0, v) \approx \begin{cases} \infty, & p = 1, \quad r > r_c, \\ f_{\text{per}}(\ln v) - \frac{r}{1-r} v^{-1}, & p = 1, \quad r < r_c, \end{cases} \quad (36)$$

where  $f_{\text{per}}(\ln v)$  is a periodic function of  $\ln v$  with period  $|\ln r|$ .

The periodic term in Eq. (36) came as a surprise to us. The large  $v$  recurrence relation (21) implies  $T(0, v) > T(0, rv)$  for  $p = 1$ , which suggests, but does not guarantee, that  $T(0, v)$  is a monotonically increasing function of  $v$ . The asymptotic form (36) for  $r < r_c$

with the periodic term is entirely consistent with  $T(0, v) > T(0, rv)$  and with Eq. (35). The periodicity already appears in the following crude approximation: For  $0 < v < v^*$  define  $T(0, v) = Av^\gamma$ , in accordance with Eq. (19), and then use the large  $v$  recurrence relation, Eq. (21) with  $p = 1$ , to obtain  $T(0, v)$  for  $v > v^*$ .

To determine  $T(0, v)$  with simulations, we measured the mean time  $T_N(0, v)$  for  $N$  boundary collisions, plotted it versus  $N^{-1}$ , and then extrapolated to  $N \rightarrow \infty$ . This is shown for  $r = 0.1$  and  $v = 0.001$  and  $0.0001$  in Fig. 3.

In Fig. 4 our results for the mean time  $T(0, v)$  for an infinite number of boundary collisions are shown as a function of  $v$  for  $p = 1$  and  $r = 0.1, 0.01$ , and  $0.001$ . For fixed  $v$  the mean time increases with increasing  $r$ , as expected.

Solving integral equation (16) reliably becomes increasingly difficult as  $r$  decreases, and in Fig. 4 we only show the numerical solution for  $r = 0.1$ . The simulation data are in good agreement with this numerical solution, with the asymptotic form (19), (20) for small  $v$ , and with the onset of periodic behavior in accordance with Eq. (36). The dashed lines for large  $v$  were calculated from the dashed lines for small  $v$  using recurrence relation (21).

## VI. CONCLUDING REMARKS

Masoliver and Porrà calculated the mean absorption time  $T(x, v)$  of a randomly accelerated particle on the finite line  $0 < x < 1$ , assuming that it is absorbed the first time it reaches either  $x = 0$  or  $x = 1$ . We have considered a more general boundary condition, parametrized by the reflection probability  $p$  and the coefficient of restitution  $r$ . We derived an integral equation which determines  $T(x, v)$  and used it to obtain the exact asymptotic form of  $T(0, v)$  for large and small  $v$  and numerical results for intermediate  $v$ . The asymptotic forms and numerical results are in excellent agreement with our computer simulations of the randomly accelerated particle.

The case  $p = 1, r < 1$  corresponds to a single particle moving between walls with which it collides inelastically. This simple and fundamental system is of interest in connection with properties of driven granular media. We find that the mean time for an infinite number of boundary collisions is finite for  $r < r_c$  and infinite for  $r > r_c$ , as predicted by Cornell *et al.* [5]. The prediction that the infinite sequence of collisions leads to inelastic collapse, with localization of the particle at the boundary, has been questioned on the basis of simulations

[17, 18] and an analysis [14] of the equilibrium distribution function  $P(x, v)$  using the same approach as in this paper. The results for the mean time reported here are largely independent of the inelastic collapse controversy. Both the integral equation and the simulation procedure sum the mean time, collision by collision, without directly addressing the question of localization at the boundary.

### Acknowledgments

We thank Jerrold Franklin for many stimulating discussions. TWB also gratefully acknowledges discussions and correspondence with Lucian Anton and Alan Bray.

### APPENDIX A: SOLUTION OF EQ. (7)

With the substitution  $\tilde{T}(x, v) = T(x, -v)$ , Eq. (7) takes the form

$$\left( v \frac{\partial}{\partial x} - \frac{\partial^2}{\partial v^2} \right) \tilde{T}(x, v) = 1 . \quad (\text{A1})$$

This differential equation is the same as Eq. (3) of Ref. [13], except for the inhomogeneous term 1 on the right-hand side. We follow Ref. [13] very closely in solving it.

First we introduce the Laplace transform

$$\tilde{Q}(s, v) = \int_0^\infty dx e^{-sx} \tilde{T}(x, v) , \quad (\text{A2})$$

which according to Eq. (A1) satisfies

$$\left( sv - \frac{\partial^2}{\partial v^2} \right) \tilde{Q}(s, v) = \frac{1}{s} + v \tilde{T}(0, v) . \quad (\text{A3})$$

This is the same as Eq. (A2) in [13], except for the extra term  $s^{-1}$  on the right-hand side. As in [13], we solve Eq. (A3) in terms of Airy functions and invert the Laplace transform, with the help of the Faltung theorem. This yields

$$\begin{aligned} \tilde{T}(x, v) = & \frac{1}{3}(\pi v)^{1/2} \int_0^x dy y^{-1/2} e^{-v^3/18y} I_{-1/6} \left( \frac{v^3}{18y} \right) \\ & + \frac{v^{1/2}}{3x} \int_0^\infty du u^{3/2} e^{-(v^3+u^3)/9x} I_{-1/3} \left( \frac{2v^{3/2}u^{3/2}}{9x} \right) \tilde{T}(0, u) \\ & - \frac{1}{3^{1/3}\Gamma(\frac{2}{3})} \int_0^x dy \frac{e^{-v^3/9(x-y)}}{(x-y)^{2/3}} \frac{\partial \tilde{T}(y, 0)}{\partial v} , \quad v > 0 , \end{aligned} \quad (\text{A4})$$

which is the same as Eq. (6) of [13], except for an additional term (the first term) on the right-hand side.

To express the unknown function  $\partial\tilde{T}(y, 0)/\partial v$  on the right-hand side of Eq. (A4) in terms of the other unknown  $\tilde{T}(0, u)$ , we first take the limit  $v = 0$  in Eq. (A4), which yields

$$\begin{aligned} \tilde{T}(x, 0) = & \frac{1}{3^{1/3}\Gamma(\frac{2}{3})} \left[ \frac{3^{2/3}}{2} \Gamma(\frac{1}{3}) x^{2/3} + x^{-2/3} \int_0^\infty du u e^{-u^3/9x} \tilde{T}(0, u) \right. \\ & \left. - \int_0^x \frac{dy}{(x-y)^{2/3}} \frac{\partial\tilde{T}(y, 0)}{\partial v} \right]. \end{aligned} \quad (\text{A5})$$

From reflection symmetry  $\tilde{T}(x, 0) - \tilde{T}(1-x, 0) = 0$ , and  $\partial\tilde{T}(y, 0)/\partial v = -\partial\tilde{T}(1-y, 0)/\partial v$ . Substituting Eq. (A5) in the first of these relations and making use of the second, we obtain

$$\int_0^1 \frac{dy}{|x-y|^{2/3}} \frac{\partial\tilde{T}(y, 0)}{\partial v} = \int_0^\infty du u \left[ \frac{e^{-u^3/9x}}{x^{2/3}} - \frac{e^{-u^3/9(1-x)}}{(1-x)^{2/3}} \right] \left( \frac{1}{2}u^2 + \tilde{T}(0, u) \right), \quad (\text{A6})$$

where we have used

$$\int_0^\infty du u^3 \frac{e^{-u^3/9x}}{x^{2/3}} = 3^{2/3} \Gamma(\frac{1}{3}) x^{2/3}. \quad (\text{A7})$$

Equation (A6) may be regarded as an integral equation for  $\partial\tilde{T}(y, 0)/\partial v$ . The solution, derived in [13] using the approach of [10, 20], is

$$\frac{\partial\tilde{T}(y, 0)}{\partial v} = \int_0^\infty du u [R(y, u) - R(1-y, u)] \left( \frac{1}{2}u^2 + \tilde{T}(0, u) \right), \quad (\text{A8})$$

where the function  $R(y, u)$  is given in Eq. (15).

Substituting Eq. (A8) in (A4) yields

$$\begin{aligned} \tilde{T}(x, v) = & \frac{1}{3}(\pi v)^{1/2} \int_0^x dy y^{-1/2} e^{-v^3/18y} I_{-1/6} \left( \frac{v^3}{18y} \right) \\ & - \frac{1}{2 \cdot 3^{1/3} \Gamma(\frac{2}{3})} \int_0^x dy \frac{e^{-v^3/9(x-y)}}{(x-y)^{2/3}} \int_0^\infty du u^3 [R(y, u) - R(1-y, u)] \\ & + \int_0^\infty du u G(x, v, u) \tilde{T}(0, u), \end{aligned} \quad (\text{A9})$$

where  $G(x, v, u)$  is given in Eqs. (14). Replacing  $\tilde{T}(x, v)$  by  $T(x, -v)$  in Eq. (A9) and evaluating the integral  $\int_0^\infty du u^3 [\dots]$ , we obtain the Green's function solution for  $T(x, -v)$  in Eqs. (13)-(15) and reproduce the Masoliver-Porrà result for  $T_1(x, v)$  in Eq. (10).

- 
- [1] H. P. McKean, J. Math. Kyoto Univ. **2**, 227 (1963).
  - [2] M. Goldman, Ann. Math. Stat. **42** 2150 (1971).
  - [3] Y. G. Sinai, Theor. Math. Phys. **90**, 219 (1992).
  - [4] T. W. Burkhardt, J. Phys. A **26**, L1157 (1993).
  - [5] S. J. Cornell, M. R. Swift, A. J. Bray, Phys. Rev. Lett. **81**, 1142 (1998).
  - [6] M. R. Swift and A. J. Bray, Phys. Rev. E **59**, R4721 (1999).
  - [7] T. W. Burkhardt, J. Phys. A **33**, L429 (2000); Phys. Rev E **63**, 011111 (2001).
  - [8] G. De Smedt, C. Godrèche, and J. M. Luck, Europhys. Lett. **53**, 438 (2001).
  - [9] T. W. Burkhardt, J. Phys. A **30**, L167 (1997).
  - [10] J. Masoliver and J. M. Porrà, Phys. Rev. Lett. **75**, 189 (1995); Phys. Rev. E **53**, 2243 (1996).
  - [11] G. Fichera, in *Boundary Problems in Differential Equations*, edited by R. E. Langer (University of Wisconsin Press, Madison, 1960); O. A. Oleinik, Sov. Math. **5**, 1129 (1964); J. N. Yang and M. Shinozuka, J. Acoust. Soc. Am. **47**, 393 (1970).
  - [12] I. S. Gradshteyn and I. M. Ryzhik, *Tables of Integrals, Series, and Products* (Academic, New York, 1980).
  - [13] T. W. Burkhardt, J. Franklin, and R. R. Gawronski, Phys. Rev. E **61**, 2376 (2000).
  - [14] T. W. Burkhardt and S. N. Kotsev, Phys. Rev. E **70**, 026105 (2004).
  - [15] Eq. (17) generalizes the result  $G(v, u) = 3(2\pi)^{-1}v^{1/2}u^{1/2}(v^3 + u^3)^{-1}$  for a particle moving on the half line  $x > 0$  with a single boundary at  $x = 0$ , derived by McKean [1] and independently by Cornell et al. [5].
  - [16] D. J. Bicout and T. W. Burkhardt, J. Phys. A **33**, 6835 (2000).
  - [17] J. Florencio, F. C. Sá Barreto, and O. F. de Alcantara Bonfim, Phys. Rev. Lett. **84**, 196 (2000).
  - [18] L. Anton, Phys. Rev. E **65**, 047102 (2002).
  - [19] This result, which may seem counter-intuitive, has the following mathematical origin: The equilibrium distribution  $P(x, v)$  obtained in [13, 14] varies asymptotically as  $P(0, v) \sim v^{-\beta(r)}$  for  $v \searrow 0$ , where the exponent  $\beta(r)$  increases monotonically from 0 to  $\frac{5}{2}$  as  $r$  decreases from 1 to 0, with  $\beta(r_c) = 2$ . Thus, the equilibrium collision rate  $I = \int_0^\infty dv v P(0, v)$  diverges at the lower limit for  $r < r_c$ . This result only holds for the continuous time dynamics (1). For

discrete dynamics with a nonvanishing time step, the number of collisions in a finite time is necessarily finite.

- [20] D. Porter and D. S. G. Sterling *Integral Equations*, (Cambridge University Press, Cambridge, 1990).



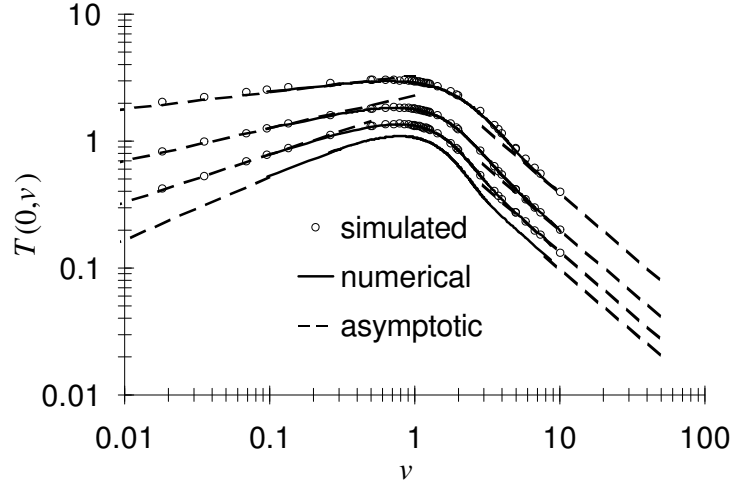


FIG. 1: Mean absorption time versus initial velocity for  $r = 1$  and, from top to bottom,  $p = 0.75$ ,  $0.50$ ,  $0.25$ , and  $0$ . The solid line for  $p = 0$  is the exact result of Masoliver and Porrà. The other solid lines are the numerical solutions of the integral equation (16). The points are the results of our simulations. The dashed lines show the exact asymptotic forms (19), (20) for small  $v$  and (22) for large  $v$ . The proportionality constant in Eq. (19) was chosen to fit the simulation data.

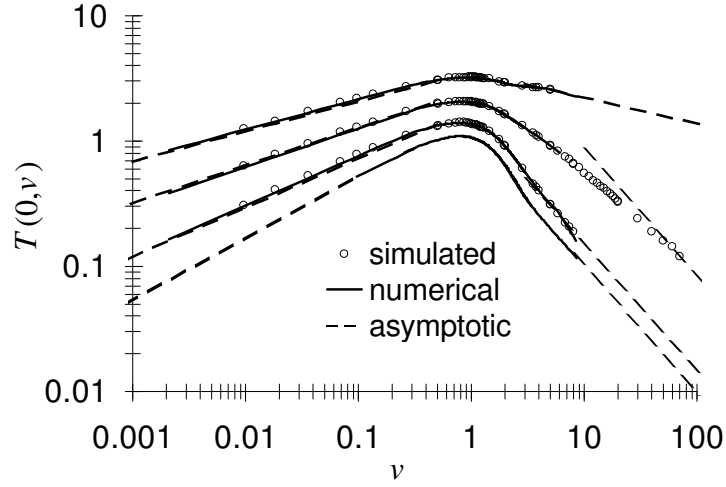


FIG. 2: Mean absorption time versus initial velocity for, from top to bottom,  $(p, r) = (0.75, 0.25)$ ,  $(0.501, 0.5)$ ,  $(0.25, 0.75)$ ,  $(0, r)$ . The bottom curve is the exact result (10) of Masoliver and Porrà. The other solid lines are the numerical solutions of the integral equation (16). The points are the results of our simulations. The dashed lines show the exact asymptotic forms (19), (20) for small  $v$  and (22) for large  $v$ . The proportionality constant in Eq. (19) was chosen to fit the simulation data. Note the slow convergence to the asymptotic form for large  $v$  for  $(0.501, 0.5)$  in the crossover region  $p \approx r$ .

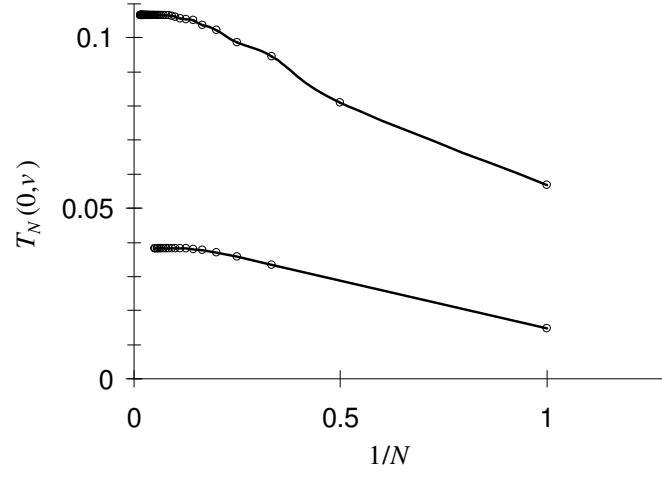


FIG. 3: Mean time  $T_N(0, v)$  for  $N$  boundary collisions versus  $N^{-1}$  for  $r = 0.01$  and, from top to bottom,  $v = 0.001$  and  $0.0001$ . The mean time  $T(0, v)$  for an infinite number of collisions is estimated by extrapolating to the vertical axis. This yields  $T(0, 0.001) = 0.108$  and  $T(0, 0.0001) = 0.039$ .

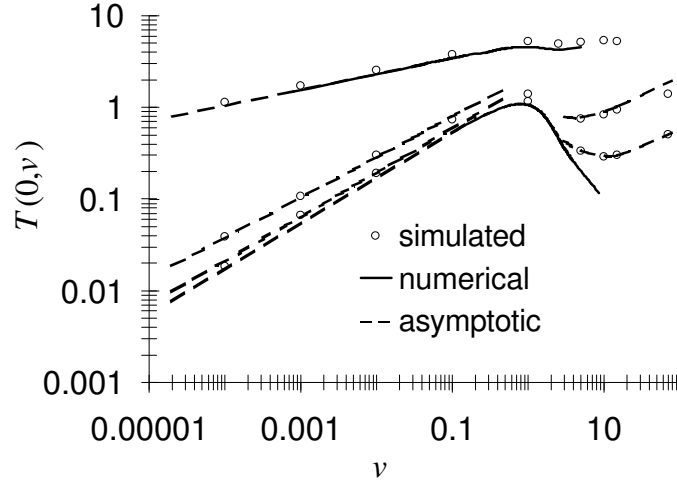


FIG. 4: Mean time for an infinite number of boundary collisions for  $p = 1$  and, from top to bottom,  $r = 0.1, 0.01, 0.001$ . The upper curve is the numerical solution of the integral equation (16) for  $r = 0.1$ . The points are the results of our simulations, obtained by extrapolation, as in Fig. 3. The bottom curve (no simulations) is the exact Masoliver-Porrà result (10). The dashed lines on the left show the exact asymptotic form (19), (20) for small  $v$ . The proportionality constant in Eq. (19) was chosen to fit the simulation data. For large  $v$ , approximately periodic behavior in  $\ln v$ , as in Eq. (36), is expected. The dashed lines for large  $v$  in Fig. 4 were calculated from the dashed lines for small  $v$  using recurrence relation (21).